LA-UR 91-4039

LA-UR--91-4039

DE92 005057

Los Alamos National Laboratory is operated by the University of California for the United States Department of Energy under contract W-7405-ENG-36

TITLE INITIAL ELECTRON-BEAM CHARACTERIZATIONS FOR THE LOS ALAMOS APEX FACILITY

AUTHOR(S) A. H. Lumpkin, R. B. Feldman, S. A. Apgar, D. W. Feldman, P. G. O'Shea

R. B. Fiorito and D. W. Rule
Naval Surface Warfare Center
Silver Springs, MD 21218

SUBMITTED TO Proceedings of the Thirteenth International Free-Electron Laser Conference, Santa Fe, NM, August 25-30, 1991

DISCLAIMER

MASTER

Los Alamos National Laboratory
Los Alamos, New Mexico 87545

"INITIAL ELECTRON-BEAM CHARACTERIZATIONS FOR THE LOS ALAMOS APEX FACILITY"[+]

A.H. Lumpkin, R.B. Feldman, S.A. Apgar,
D.W. Feldman, P.G. O'Shea
Los Alamos National Laboratory
and
R.B. Fiorito and D.W. Rule
Naval Surface Warfare Center
Silver Springs, MD 21218

Abstract

The ongoing upgrade of the Los Alamos Free-Electron Laser (FEL) Facility involves the addition of a photoelectric injector (PEI) and acceleration capability to about 40 MeV. The electron-beam and high-speed diagnostics provide key measurements of charge, beam position and profile, divergence emittance, energy (centroid, spread, slew, and extraction efficiency), micropulse duration, and phase stability. Preliminary results on the facility include optical transition radiation interferometer measurements of divergence (1 to 2 mrad), FEL extraction efficiency (0.6 ± 0.2%), and drive laser phase stability (<2 ps [rms]).

[+]Work supported by the U.S. Strategic Defense Initiative under the auspices of U.S.DOE.

I. INTRODUCTION

The continuing upgrade of the Los Alamos Free-Electron Laser (FEL) Facility now encompasses the photoelectric injector (PEI) installed last year[1] and two additional accelerator tanks and an FEL resonator installed in the past year.[2] This facility is now considered part of the Average Power Laser Experiment (APLE) program. It is specifically charged to serve as the APLE Prototype Experiment (APEX). The electron-beam diagnostics have been extended along with the accelerator beamline. These e-beam diagnostics provide key measurements of charge, beam position and profile, divergence, emittance, energy (centroid, spread, slew, and extraction efficiency), micropulse duration, and phase stability. Many of the time-resolved diagnostics are based on gated/ intensified cameras and/or streak cameras. Electron beam information is converted to visible images via optical transition radiation (OTR), Cerenkov radiation (CR), synchrotron radiation (SR), and spontaneous emission radiation (SER). Additionally, the streak camera has been used to characterize the PEI drive laser at the fundamental and the doubled-frequency components. Preliminary measurements include OTR interferometer results on divergence, CR imaging results from the spectrometer involving extraction efficiency, and drive laser phase stability measurements. Some of the future diagnostic development plans on APEX are also discussed.

II. EXPERIMENTAL PROCEDURES AND BACKGROUND

As a basic background Fig. 1 shows a schematic of the APEX beamline configuration. Several of the diagnostic stations are also indicated. In the accelerator section there is an OTR profile monitor after each accelerator tank. At these first four stations there is also a wall current monitor (WCM) for measuring charge noninterceptively. In the middle of the 60^{o} bend there is a view screen in the energy dispersed location. The resonator leg includes one station before the wiggler (#6), one station in the middle of the wiggler (#7), one station at the end of the wiggler (#8), and spectrometer #1. The 150^{o} bend diagnostics have been designed, but that beamline is not yet completed. It is also noted that at present there is an OTR interferometer at station #4 viewed by our standard two-camera beamspot/divergence diagnostics.[3] Both of these cameras are gated, intensified charge-injection-device (ICID) systems. Stations 1-4 and the spectrometer all involve intensified cameras which provide sufficient sensitivity to image a single micropulse with a charge of a few nanocoulombs.

In Table I we summarize the basic ten parameters addressed, the nominal value, span, measuring technique, resolution, error, and timescale of interest. As an example divergences are anticipated in the 0.5 - 3.0 mrad span, and we intend to use the OTR interferometer. This technique takes advantage of the rather unique properties of optical transition radiation which have been described previously.[4]

Very briefly Fig. 2 shows a schematic of such a device. The forward TR from the first foil interferes with the backward TR from foil #2 to produce an interferogram that is energy and divergence dependent. In particular the fringe visibility is relatable to the divergence of the beam and the opening angle of the distribution is related to the reciprocal of the Lorentz factor (gamma). In our experiments last year at 15-17 MeV we used an interfoil spacing of only 1.4 mm and had to look through the first foil (1.1 μm of Kapton). This configuration required the inclusion of coherent amplitudes from the first foil in the analysis.[5] With the higher γ this year, we explored a spacing of 15 mm (when rotated 45°) that would allow the direct viewing of the interference pattern at the surface of the second foil. Figure 3 shows the calculated fringe pattern for E=40 MeV, a 50-nm bandpass filter, and rms divergences of 0.63 mrad and 1.76 mrad. Additional sensitivity to lower divergences can be obtained by using only a 10-nm wide bandpass filter as shown in Fig. 4. In these cases we actually look at the projections on the x- or y-axis. If we measure both the spot size and the divergence while providing a beam waist at this axial location, emittance can be determined. After the 60° bend we used two- or three-screen profile measurements to determine emittance.

Although we directly measured e-beam micropulse bunch length last year as well as that of the drive laser[6], this year's experiments have relied mainly on the drive laser measurements. A Hamamatsu C1587 streak camera forms the basis

of these measurements. In particular, we have used a synchroscan module that is phase-locked to the reference 108.3 MHz rf oscillator signal to test phase stability of the drive laser. Simulations are then used to estimate the effects on e-beam parameters. An optical transport path is under design that would transport OTR, CR, or SR, radiation to the streak camera's present location in the drive laser room.

III. RESULTS AND DISCUSSION

Preliminary results during the commissioning of 34-40 MeV operations, initial lasing with the high quantum efficiency photocathode, and samples of the drive laser studies are now presented.

Following the initial steps of accelerating and transporting the electron beam around the 60° bend, through the wiggler, and to the spectrometer/beam dump, we concentrated on producing initial lasing. Various trades in e-beam parameters were evaluated, and we decided on accepting approximately 100A peak current, 37-MeV energy, 100-150 π mm-mrad emittance, and an energy spread of 1 to 2% for lasing in the 3.5-3.8 μm regime. This would result in small-signal gains of only 15-20% based on simulations, but this was a trade. During the lasing trials the photocathode was irradiated with a full Gaussian intensity variation across its 10-mm diameter. As shown in Fig. 5, the projected rms divergence on the x-axis was approximately 2 mrad as compared to the measured 1 mrad for a truncated Gaussian laser irradiation with 4-mm diameter. Operation time of 1 nC per micropulse was extended by using the full cathode irradiation

at a sacrifice to beam divergence and emittance. It is noted that the fringe visibility was less than the calculated case at 0.63 mrad in Fig. 3.

During lasing operations on June 21, 1991, the FEL extraction efficiency was monitored by the electron beam spectrometer after the wiggler. Figure 6 shows the macropulse average energy spectral image for nonlasing (upper) and lasing (lower) conditions. The low-energy electron tail (to the left) due to lasing is clearly visible. Profiles taken along the energy axis (horizontal) of the image are processed and compared in Fig. 7. The net centroid shift of the two spectra is shown to be 0.6 $\pm$ 0.2%. The integrated counts under the curves were within 12% of each other for a window taken through the central region and within 5% for the box-average window sample over the whole images. This integral balance indicates similar electron-beam operations and transport occurred, and the video system response is reasonable. The optical diagnostics on the FEL were not prepared to provide extraction efficiency results at this time. However, the subsequent inspection of the cavity, mirrors showed the damage threshold had beam exceeded for the multi layer dielectric coatings which qualitatively corroborated the 1/2% extraction efficiency regime.[7] Additionally, simulations of the experimental conditions by J.C. Goldstein shown in Fig. 8 for optical power and extraction efficiency versus pass number are in reasonable agreement with the experimental value.[8] For our almost 40-period wiggler we achieved almost one-half the

theoretical limit even with this beam quality and limited operation time.

As a preliminary to the electron-beam characterizations, the PEI drive laser was characterized for phase stability as described by Lumpkin and Early in these proceedings.[9] Here we briefly point out the assessment of the Nd:YLF master oscillator by viewing the pulse-compressed 1.05 μm radiation with the synchroscan streak camera. In the upper image of Fig. 9 the 20-event computer sum of the laser macropulses clearly shows the blurred structure with a bunch length of 18.4 ps (FWHM) when the mode locker becomes unstable. This is compared to the lower image of a single macropulse (synchroscan sum over its 400 micropulses) with an observed bunch length of only 10.5 ps (FWHM). Table III expands on this by showing a series of tests where the phase stabilizer and the amplitude stabilizer were active or inactive. Observed bunch lengths for one macropulse versus about 20 were used to estimate the effective intermacropulse jitter. The best results (approximately 1 ps rms jitter) were obtained with both stabilizers active for both the 7 ps and 12.6 ps autocorrelator-determined IR bunch length. The streak camera determined bunch lengths of 7.8 and 11.4 ps, respectively, are in reasonable agreement. It is noted that the mechanical shutter provided about a 1-ms long macropulse at 108.3 MHz micropulse repetition rate. Studies of the doubled-frequency

component at 21.7 MHz repetition rate and a 20-μs macropulse tended to show more jitter in the experiments, but these were done with a different camera.

Planned development activities at APEX in support of the APLE program in the next year include:

- o the investigation of synchrotron radiation source strengths at low gamma (<100) for potential nonintercepting beam position, profile, divergence, and micropulse length diagnostics (see Ref. 10, these proceedings)
- o investigations of spontaneous emission radiation harmonics (for potential beam profile, position, energy, and micropulse length diagnostics
- o test of the prototype beam position monitor for the elliptical bore APLE wiggler, and
- o test of the flying wire prototype for beam position and profile samples

IV. SUMMARY

In summary, all base electron-beam diagnostics on the APEX oscillator configuration are operational. We have demonstrated the viability of the OTR interferometer design for "looking between the foils" at energies of 35-40 MeV. Preliminary extraction efficiency results from the new spectrometer have been obtained that are about one-half the theoretical limit for an ideal beam. In the next year, we anticipate building our data base on the APEX parameters, optimizing the emittance before and after the bends (transport

of bright beams), and executing the development program described above.

V. ACKNOWLEDGMENTS

The authors wish to thank T. Zangs, J. Barton, P. Schafstall, J. Early, and W. Stein for APEX operation support; N. Iksanoto, M. Feind, D. Byrd, and S. Bender for specific APEX beamline laser alignment support; and M. Schmitt, B. Carlsten, and J. Goldstein for theoretical simulations support.

REFERENCES

1. D.W. Feldman, et al., Nucl Inst. and Methods in Physics Res., A304, 1991, 224.
2. P.G. O'Shea, et al., "Initial Results from the Los Alamos Photoinjector-Driven Free-Electron Laser," Proceedings of the 13th International Free-Electron Laser Conference, Santa Fe, NM, August 25-30, 1991.
3. A.H. Lumpkin, et al., Nucl Inst. and Methods in Physics Res., A285 (1989) 343.
4. L. Wartski, et al., J. Appl. Physics, 46, 1975, 3644.
5. D.W. Rule, et al., Nucl. Inst. and Methods in Physics Res., A296 (1990) 739.
6. Alex H. Lumpkin, Bruce E. Carlsten, and Renee B. Feldman, Nucl. Inst. and Methods in Physics Research, A304 (1991) 374.
7. S.C. Bender, (Los Alamos National Laboratory), private communication, June, 1991.

8. J.C. Goldstein, (Los Alamos National Laboratory), private communication, July, 1991.

9. Alex H. Lumpkin and James W. Early, "First Dual-Sweep Streak Measurements of a Photoelectric Injector Drive Laser", These Proceedings.

10. Robert B. Greegor and Alex H. Lumpkin, "Synchrotron Radiation as a High-Power Diagnostic Concept for the Average Power Laser Experiment (APLE)," These Proceedings.

FIGURE CAPTIONS

Fig. 1. A schematic of the APEX master oscillator power amplifier configuration with a number of the diagnostic stations indicated.

Fig. 2. Schematic of the OTR interferometer. In this case the first foil is 0.8 um of Al separated by 11mm from the aluminized fused silica.

Fig. 3. Calculated interference patterns for rms beam divergence of 0.63 and 1.76 mrad. Since the interferometer is at 45^{o} to the beam effective separation is 15.6 mm. The bandwidth filter is 50-nm wide.

Fig. 4. Calculated interference patterns for rms beam divergences of 0.63 mrad and 0.26 mrad and a 10-nm wide bandpass filter.

Fig. 5. Measured e-beam divergences for drive laser irradiations on the photocathode of 10-mm and 4-mm diameter.

Fig. 6. Electron-beam spectrometer images showing the effects of lasing on the observed spectra.

Fig. 7. Energy profile analysis of the images in Fig. 6 used to determine extraction efficiency.

Fig. 8. Simulations of FEL performance with the approximate e-beam conditions of the experiment (provided by J.C. Goldstein).

Fig. 9. Synchroscan streak images of the Nd:YLF drive laser fundamental illustrating the phase instability when the mode locker is unstable for a 20-event macropulse integration (upper) compared to the single macropulse (lower).

Table I. Electron Beam Parameters and their Diagnostics (APEX)

Parameter	Nominal Value	Span	Technique	Resolution	Error	Timescale
Position	Reference to Laser Line	± 10 mm	OTR Screens	~ 50 μm	~ 100 μm	Single - Micro or Streak
Transverse Profile	1 mm, FWHM	0.5 - 15 mm	OTR Screens	~ 50 - 100 μm	5 - 10%	Single - Micro or Streak
Divergence	1 - 2 mrad	0.5 - 3.0 mrad	Two-Station OTRI	Few Tenths mrad 0.4 mrad Limiting	15% 15%	Single - Micro Macro
Emittance	50 π mm - mrad	60 - 150 π	Two Station OTRI	Depends On Beam Transport	(30%) (30%)	Single - Micro Macro
Pointing	On Laser Line	0 - 5 mrad	OTRI Two-Station	~ 0.2 mrad ~ 0.2 mrad	20 - 30%	Submacro
Charge	5 nC	0 - 10 nC	Wall Current Monitor	0.1 nC	20%	Submacro
Energy	40 MeV	6 - 45 MeV	Spectrometer	~ 0.2%	(10%)	Submacro
Spread	0.5%		90° Bend,			
Jitter	± 0.2%		Cherenkov			
Slew	0.24%		Screen			
Micropulse Duration	15 - 20 ps	5 - 35 ps	Streak Camera Cherenkov rad	2 ps (fast) 6 ps (synchro)	10 - 15%	Submicro
Drive Laser	10 - 15 ps	5 - 35 ps	Streak Camera	2 ps (fast)	10 - 15%	Submicro
Jitter			Synchroscan	4 ps Over Seconds		
Slew			Synchroscan	< 4 ps Over Seconds		
Beam Spill	Relative to No Beam	—	X-Ray Detector	Field Emission		Submacro

Table II. Summary of Preliminary Emittance Results (macropulse average)

Date	Set #	Condition (diam PC)	Beam Diameter FWHM (mm)	rms-Divergence (mrad)	Emittance (πmm-mrad)
6-24-91	1	10 mm	0.82	2.0	205
	2	6 mm	0.69	1.1	95
	5	4 mm	0.81	1.0	102

Table III. Summary of Preliminary Streak Camera Results on APEX Master Oscillator Pulse Length and Phase Stability ($\lambda = 1.05\ \mu m$)

Stabilization Conditions		Total Pulse Length (FWHM) (ps)	Macropulse Ave Pulse Length* (FWHM) (ps)	Autocorrelator Pulse Length (FWHM) (ps)	Number of Macropulses**	Intermacropulse Jitter (ps)	
Phase	Amplitude					FWHM	rms
Yes	Yes	10.4	7.8	7	1	--	--
No	Yes	10.1	7.4	7	1	--	--
Yes	Yes	10.1	7.4	(7)	20	<1	<1
No	Yes	13.0	7.4	7	20	8	3.4
Yes (modelocker unstable)	Yes	18.4	(7.4)	(7)	20	15	6.4
Yes	Yes	13.4	11.4	12.6	1	--	--
Yes	Yes	13.8	11.4	12.6	20	≤3	≤1
No	Yes	17.8	11.4	12.6	20	11.2	4.8

* Limiting streak camera resolution [≤6 ps (FWHM)] and jitter [4 ps (FWHM)]

** Macropulse ~1 ms long from mechanical shutter, 108 MHz micropulse repetition rate

Schematic of APEX
Master Oscillator Power Amplifier (MOPA)

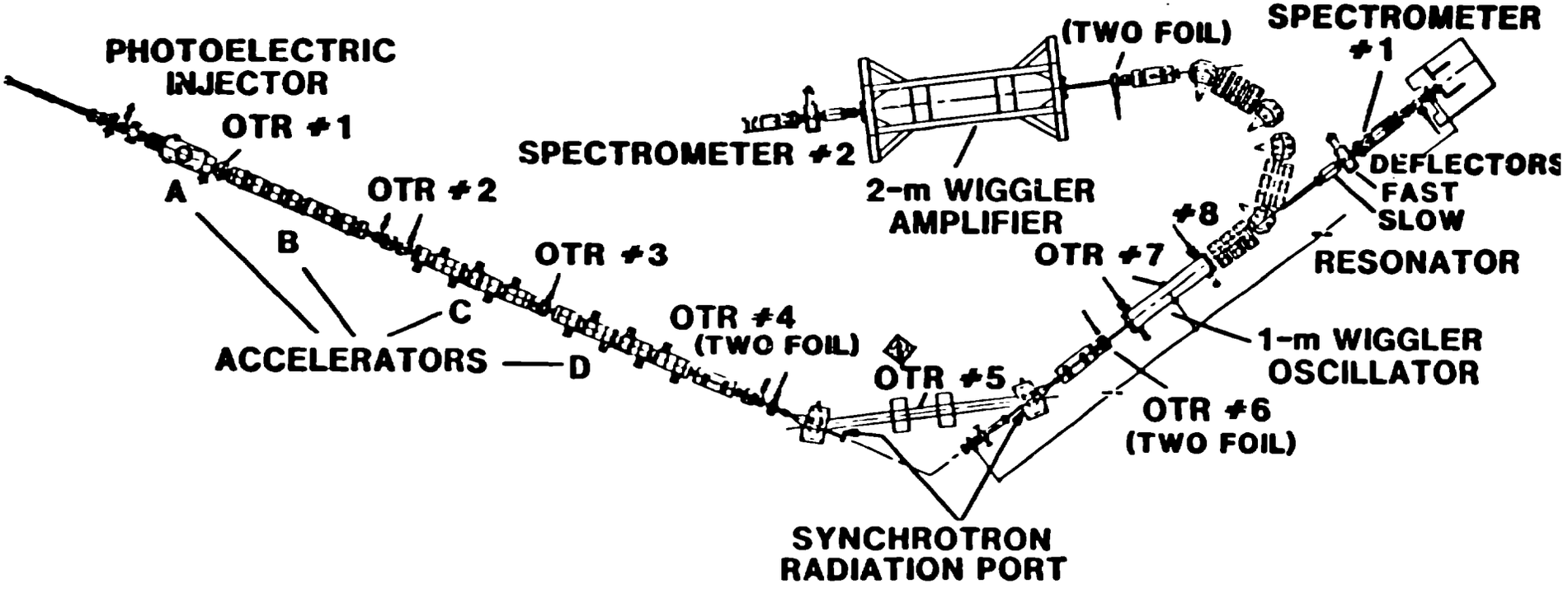

Fig. 1.

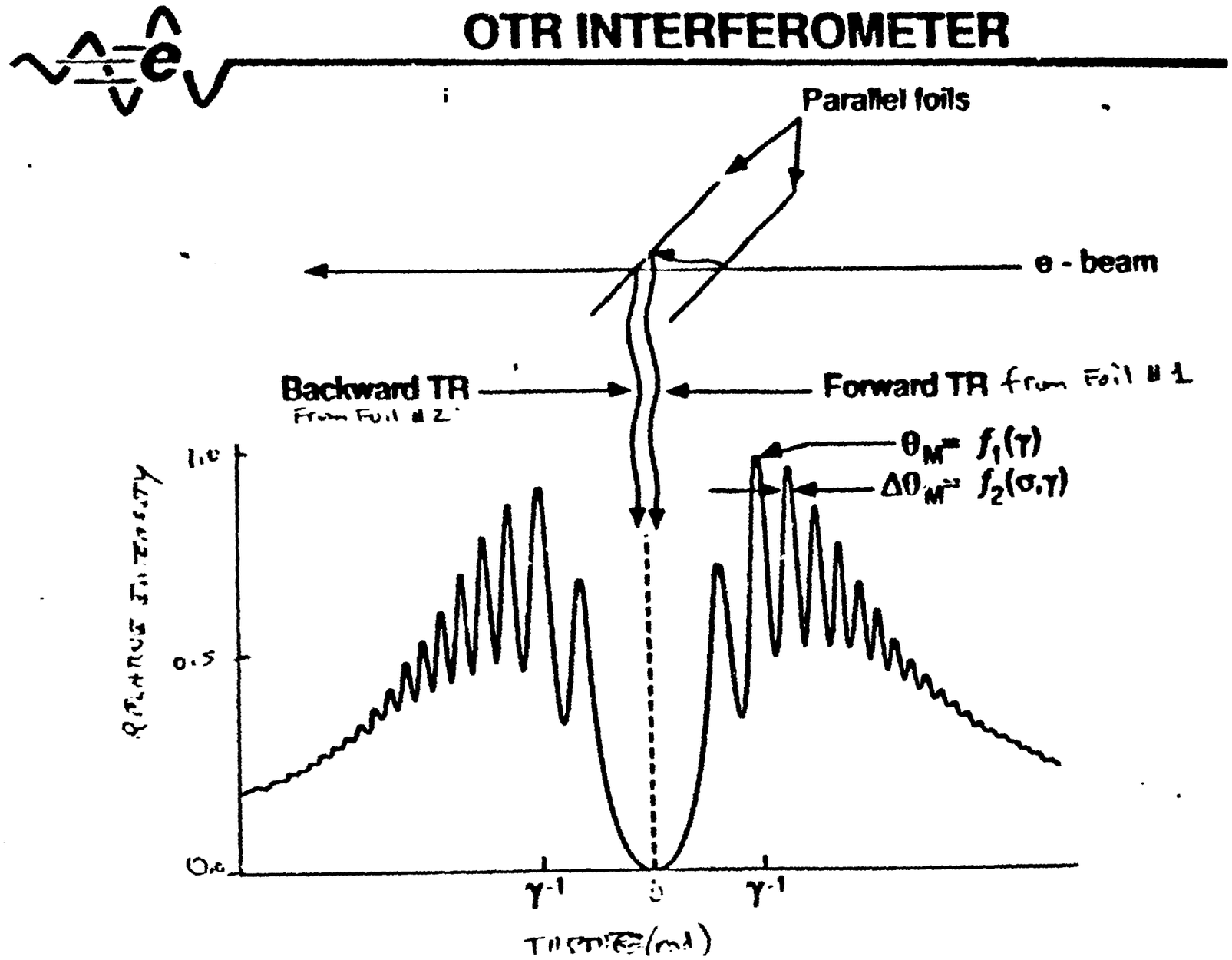
OTR INTERFEROMETER
Parallel foils
e - beam
Backward TR
From Foil # 2
Forward TR from Foil # 1
$\theta_M \approx f_1(\gamma)$
$\Delta\theta_M \approx f_2(\sigma,\gamma)$
1.0
0.5
0.0
γ^{-1}
0
γ^{-1}

Fig. 2.

INTERFEROMETER DESIGNED TO ASSESS ~0.5 mrad DIVERGENCES (θ_{rms}) (without clear foil term)

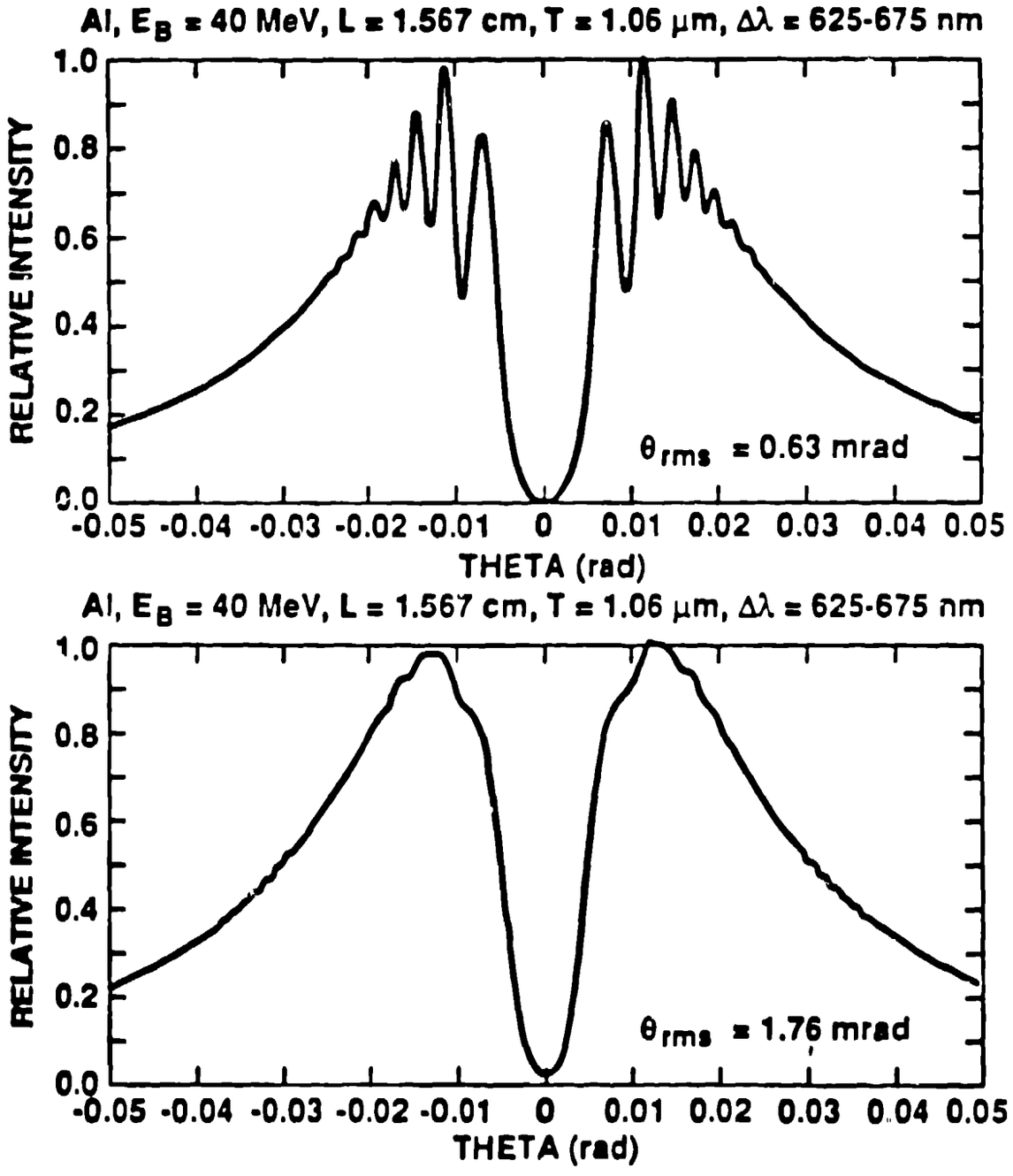

P-15/NL-41

Fig. 3.

F3

10-nm BANDWIDTH FILTER ENHANCES SENSITIVITY OF INTERFEROMETER TO ASSESS ~0.5 mrad DIVERGENCES (θ_{rms})

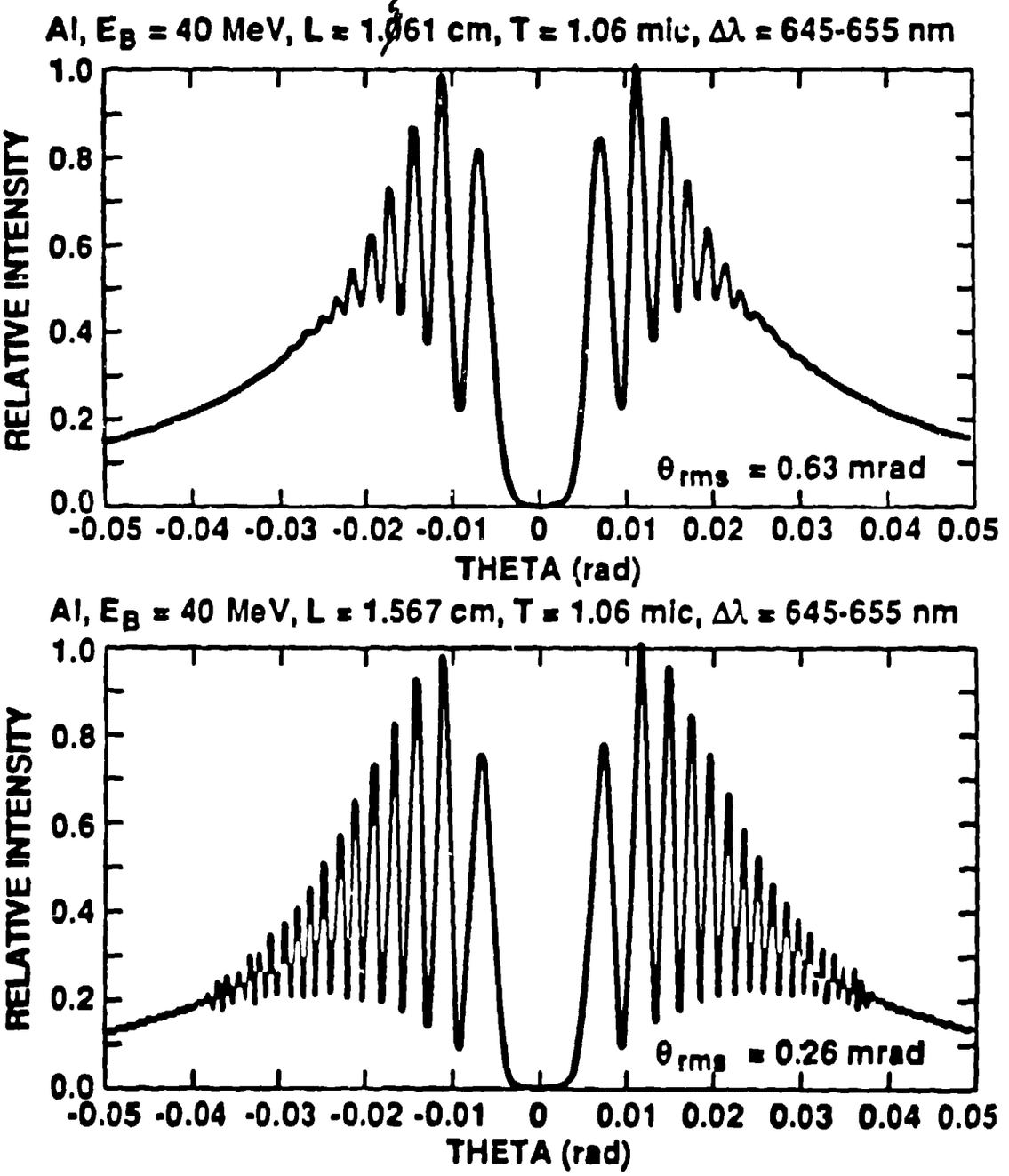

DIVERGENCE DECREASED WITH TRUNCATION OF DRIVE LASER PROFILE (6-24-91)

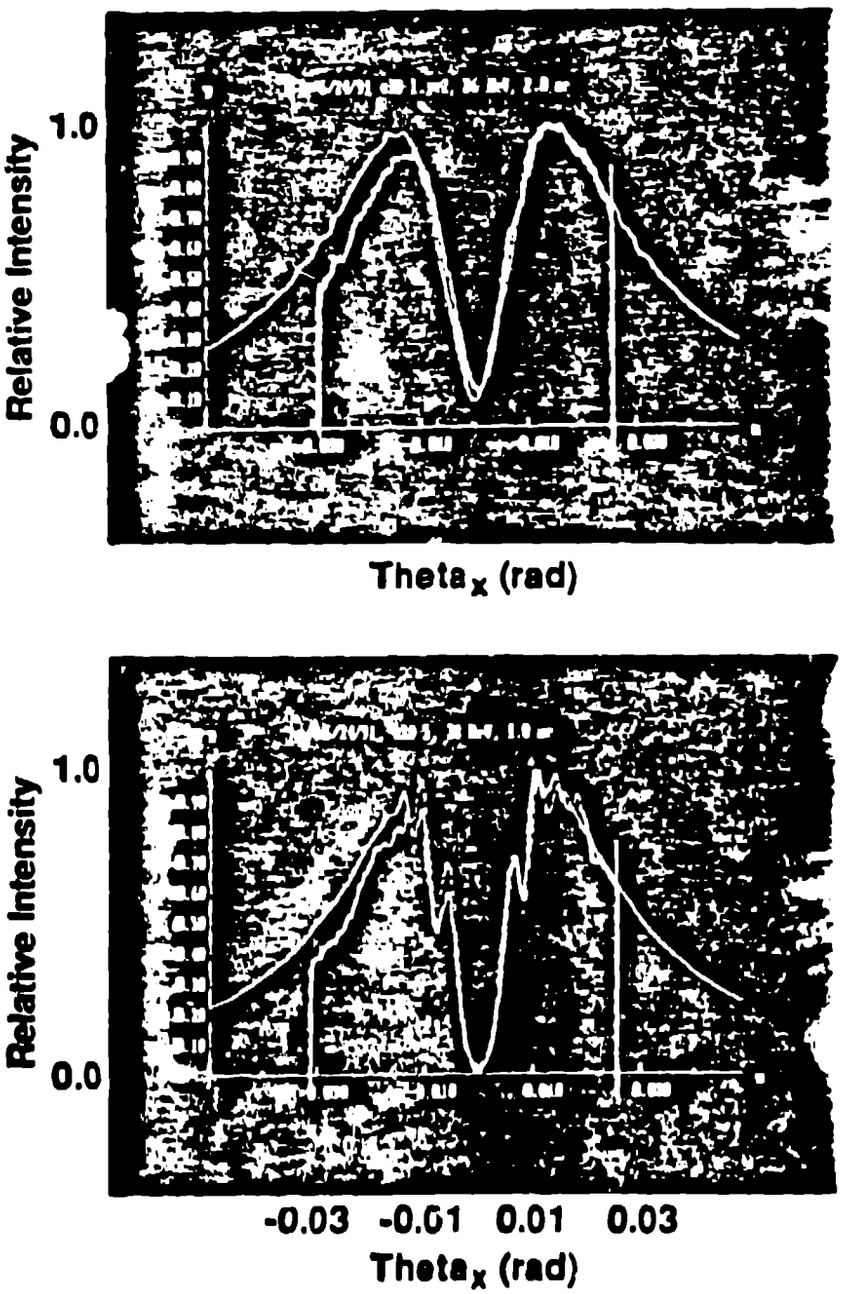

Fig. 5.

Significant Extraction Efficiency Observed in E-beam Spectrometer on First Day of Lasing at APEX (6 - 21 - 91)

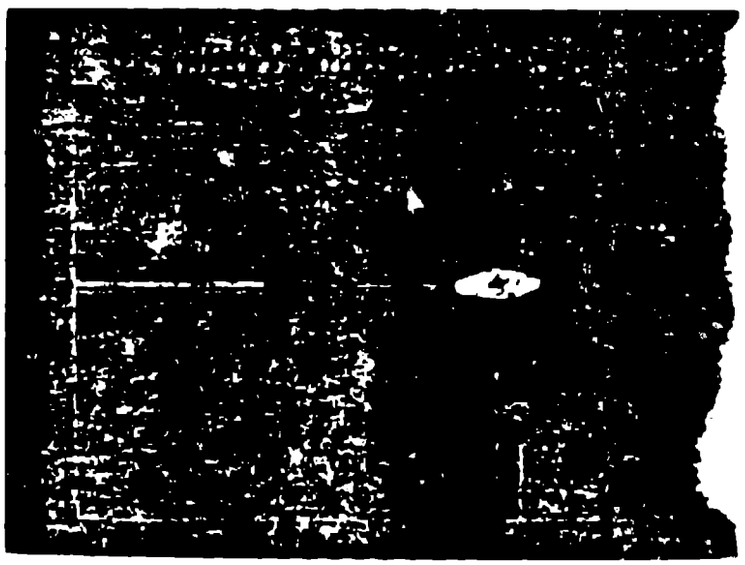

NO LASING

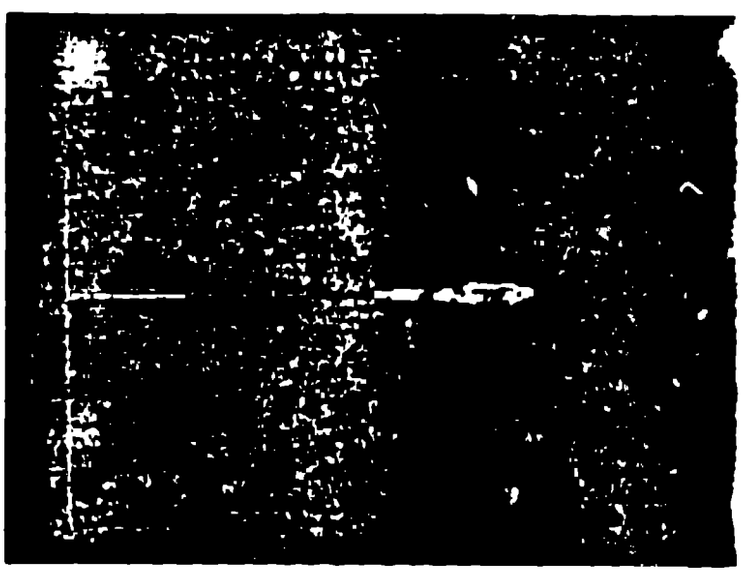

LASING

Energy Increasing ⟶

Fig. 6.

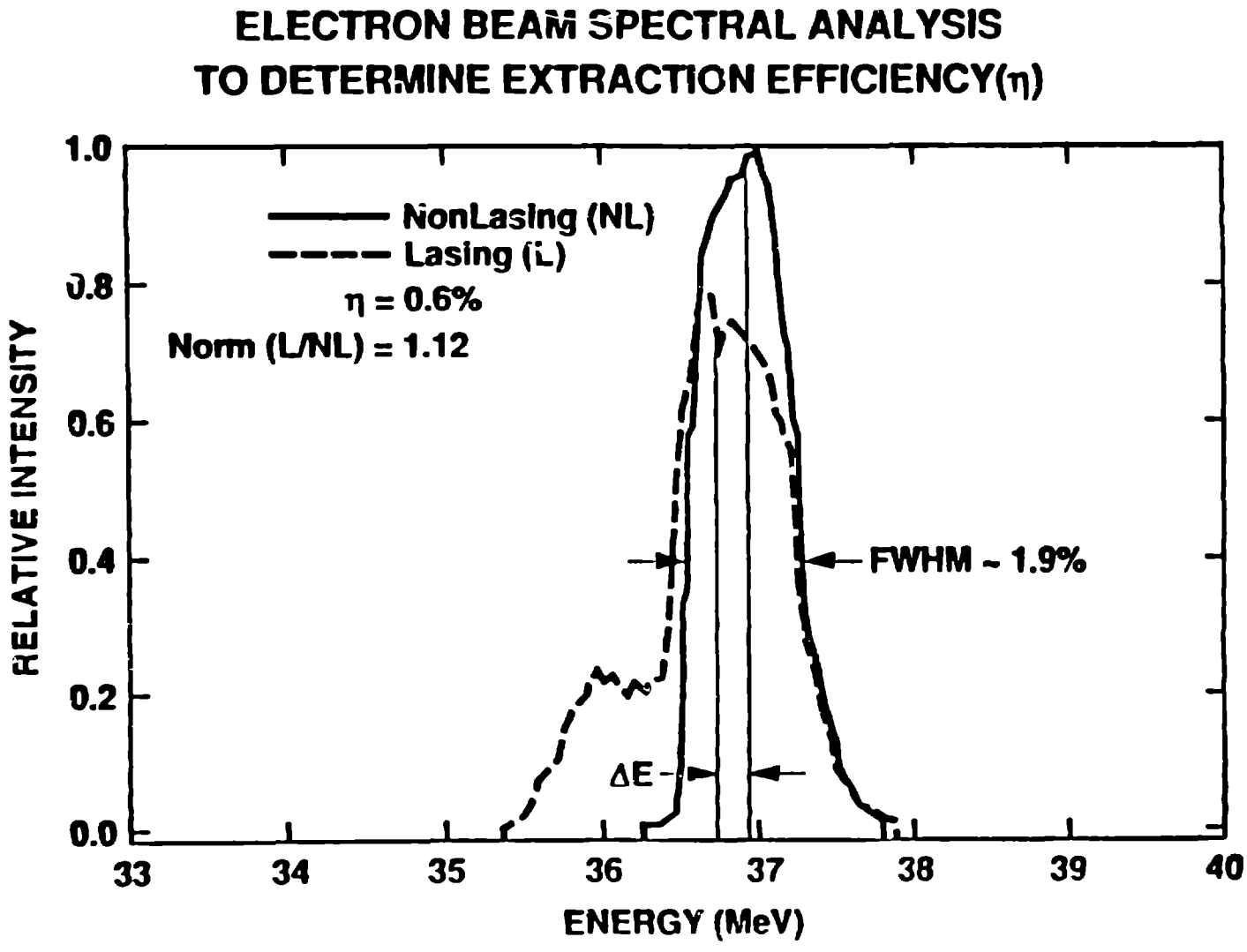
ELECTRON BEAM SPECTRAL ANALYSIS
TO DETERMINE EXTRACTION EFFICIENCY(η)
NonLasing (NL)
Lasing (L)
η = 0.6%
Norm (L/NL) = 1.12
FWHM ~ 1.9%
ΔE
RELATIVE INTENSITY
ENERGY (MeV)
1.0
0.8
0.6
0.4
0.2
0.0
33
34
35
36
37
38
39
40

Fig. 7.

FEL SIMULATIONS OF EXPERIMENT IN AGREEMENT WITH INITIAL RESULTS (Optical Power and Extraction Efficiency)

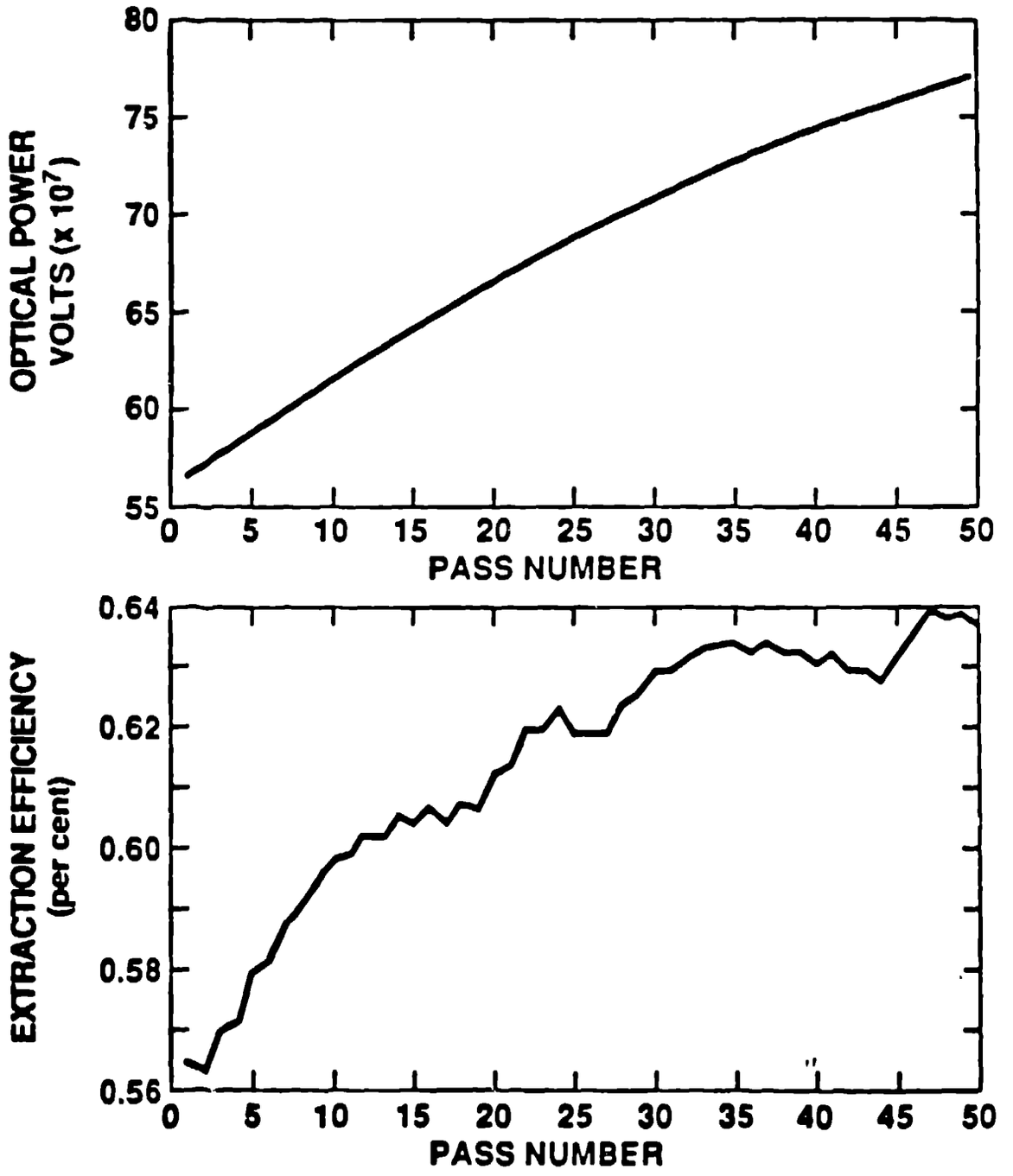

Courtesy J. C. Goldstein

Fig. 8.

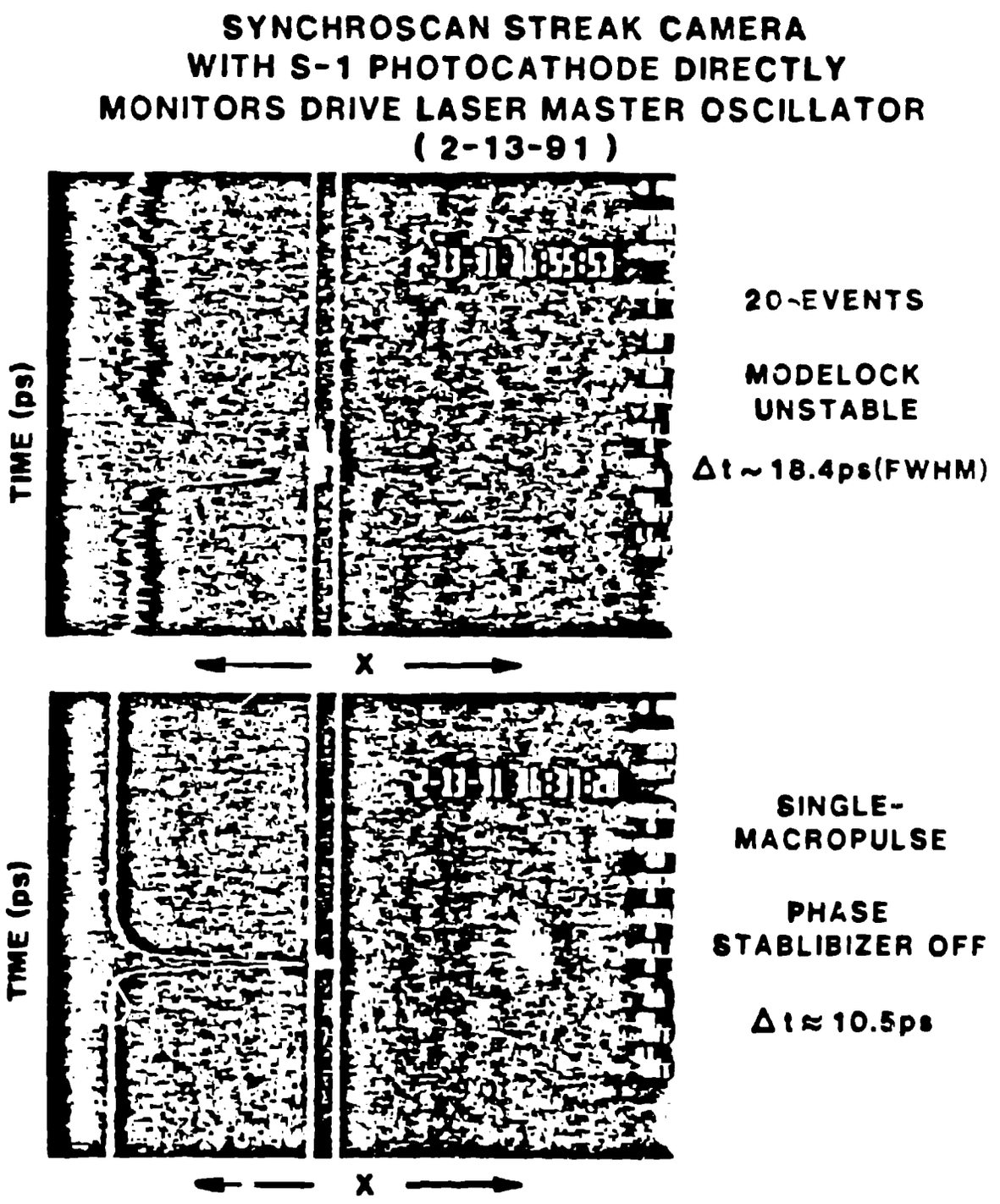
SYNCHROSCAN STREAK CAMERA
WITH S-1 PHOTOCATHODE DIRECTLY
MONITORS DRIVE LASER MASTER OSCILLATOR
(2-13-91)
TIME (ps)
X
20~EVENTS
MODELOCK
UNSTABLE
Δt ~ 18.4ps(FWHM)
TIME (ps)
X
SINGLE-
MACROPULSE
PHASE
STABLIBIZER OFF
Δt ≈ 10.5ps

Fig. 9.